

# Synthesis, characterization and catalytic activity of Nd<sub>2</sub>O<sub>3</sub> supported V<sub>2</sub>O<sub>5</sub> catalysts

S. Shylesh<sup>1</sup>, T. Radhika, K. Sreeja Rani, S. Sugunan\*

*Department of Applied Chemistry, Cochin University of Science and Technology, Cochin 686022, India*

Received 29 January 2005; received in revised form 21 March 2005; accepted 15 April 2005

## Abstract

A series of rare-earth neodymia supported vanadium oxide catalysts with various V<sub>2</sub>O<sub>5</sub> loadings ranging from 3 to 15 wt.% were prepared by the wet impregnation method using ammonium metavanadate as the vanadium precursor. The nature of vanadia species formed on the support surface is characterized by a series of different physicochemical techniques like X-ray diffraction (XRD), Fourier transform infrared spectroscopy (FTIR), BET surface area, diffuse reflectance UV–vis spectroscopy (DR UV–vis), thermal analysis (TG-DTG/DTA) and SEM. The acidity of the prepared systems were verified by the stepwise temperature programmed desorption of ammonia (NH<sub>3</sub>-TPD) and found that the total acidity gets increased with the percentage of vanadia loading. XRD and FTIR results shows the presence of surface dispersed vanadyl species at lower loadings and the formation of higher vanadate species as the percentage composition of vanadia is increased above 9 wt.%. The low surface area of the support, calcination temperature and the percentage of vanadia loading are found to influence the formation of higher vanadia species. The catalytic activity of the V<sub>2</sub>O<sub>5</sub>-Nd<sub>2</sub>O<sub>3</sub> catalysts was probed in the liquid phase hydroxylation of phenol and the result show that the present catalysts are active at lower vanadia concentrations.

© 2005 Elsevier B.V. All rights reserved.

*Keywords:* Neodymia; Vanadia; Orthovanadate; Phenol hydroxylation

## 1. Introduction

Metal oxide supported vanadia catalysts are the basic component of several industrial catalysts, which are used for the selective oxidation and ammoxidation of various hydrocarbons and for the selective catalytic reduction of NO<sub>x</sub> with NH<sub>3</sub> [1–5]. The catalytic activity of vanadia species depends largely on the nature of the support, as support interaction usually affects the dispersion and redox properties of the active vanadia phases and hence shows differences from bulk V<sub>2</sub>O<sub>5</sub>. Furthermore, from a reaction point of view, it has been well documented that the selectivity and activity of these supported vanadia catalysts depends on the acid–base properties of the support, calcination temperature and percentage

of vanadia loading apart from its surface acidity. Thus, careful choice of the support, suitable preparation procedure, precise amount of vanadia loaded seems to be the crucial factors in the preparation of vanadia catalysts for a definite reaction. The interesting characteristic properties of vanadia-ceria catalysts [6,7] and its impact in the heterogeneous catalysis scenario focused tremendous attention towards various rare-earth supported vanadia catalysts.

The existence of different surface vanadium oxides on various single oxide supports (TiO<sub>2</sub>, SiO<sub>2</sub>, MgO and CeO<sub>2</sub>) and mixed oxides (TiO<sub>2</sub>-SiO<sub>2</sub> and TiO<sub>2</sub>-Al<sub>2</sub>O<sub>3</sub>) has undergone considerable research and refinement during the last few decades since the properties of bulk vanadia is entirely different on a support. Rare-earth supported vanadia catalysts find extensive applications in recent years especially with cerium, since the presence of Ce<sup>4+</sup>/Ce<sup>3+</sup> redox couple made them genuinely interesting in the selective partial oxidation of various hydrocarbons. Au et al. [8,9] reported the preparation of different rare-earth orthovanadates

\* Corresponding author. Tel.: +91 484 2575804; fax: +91 484 2577595.

*E-mail address:* [ssg@cusat.ac.in](mailto:ssg@cusat.ac.in) (S. Sugunan).

<sup>1</sup> Present address: Catalysis Division, National Chemical Laboratory, Pune 411008, India.

and had verified its catalytic activity in the oxidative dehydrogenation reaction of propane. However, literature reveals that reports on vanadia–neodymia mixed oxides are scarce, and hence, it is interesting to evaluate its surface properties and to screen its activity towards different selective oxidation reactions.

Diphenols like catechol and hydroquinone are important chemical materials especially in agro chemical and fine chemical industries. Formation of diphenols from phenol hydroxylation using  $\text{H}_2\text{O}_2$  as oxidant has become one of the promising approaches due to its minimum environmental pollution, high active oxygen content and the absence of any toxic by-products. This oxidation process is frequently reported as taking place through the decomposition of  $\text{H}_2\text{O}_2$  with the formation of an unstable electrophilic intermediate, which attacks the phenol nucleus to give a phenoxy ion. The catalysts prepared till date for this reaction are the high surface area titanosilicates [10], molybdovanadophosphates [11], metal complexes [12,13] etc., but had the drawbacks like the difficulty in the separation of catalysts from products, complicated preparation procedure and low product yields. Moreover, literature reveals that simple metal oxides and supported metal oxides like  $\text{Fe}_2\text{O}_3$  [14],  $\text{MoO}_3$  [15],  $\text{V}_2\text{O}_5$  and  $\text{TiO}_2$  colloidal particles [16] and materials with low surface area catalysts like V-Zr-O, Cu-Bi-V-O were active for the hydroxylation of phenol in presence of  $\text{H}_2\text{O}_2$  [17,18].

In the present report, we present our results on the interaction of vanadia species at different loadings with the rare-earth neodymia using a series of different characterization techniques. We extend our studies further to elucidate the nature of vanadia species present in the different loaded samples, its interaction with the support and its role in the phenol hydroxylation reaction. Catalytic data show that the supported catalysts can promote the hydroxylation of phenol to a suitable extent and are stable under the reaction conditions opted.

## 2. Experimental

### 2.1. Catalyst preparation

The incipient wet impregnation method was opted to prepare the vanadia-neodymia catalysts used in the study. The support neodymia was prepared via hydroxide method by precipitation from its nitrate solution (neodymium nitrate, supplied by Indian Rare Earth Ltd., Udyogamandal, Kerala) by the dropwise addition of 1:1 ammonia. The resultant mass obtained was then made free from nitrate ions and evaporated in a water bath kept at  $110^\circ\text{C}$  for 12 h. The support was calcined in air at  $500^\circ\text{C}$  prior to impregnation with an aqueous solution containing ammonium metavanadate (supplied by Merck Chemicals) and oxalic acid in a 1:2 molar ratio. The percentage of vanadium and total amount of impregnating solution were adjusted in order to produce catalysts with

vanadium weight loading between 3 to 15 wt.% [19]. The samples were then dried overnight at  $100^\circ\text{C}$  and finally calcined in air at  $500^\circ\text{C}$  for 5 h. The catalysts were named according to the weight percentage of vanadia loading and its calcination temperature (for example, the sample 6VN/500 means that 6 wt.% of vanadia was loaded on the support and calcined at a temperature of  $500^\circ\text{C}$ ). An  $\text{NdVO}_4$  sample had been also prepared to check the formation of orthovanadate species at higher loadings and thus considered as a reference compound.

### 2.2. Characterization

The phase compositions of the prepared catalysts were identified on Rigaku D-Max X-Ray Diffractometer equipped with a Ni filtered  $\text{Cu K}\alpha$  radiation at room temperature in the  $2\theta$  range of  $10^\circ$ – $60^\circ$ . IR spectroscopy studies were carried with a Jasco FTIR-5300 instrument in the range of  $4000$ – $400\text{ cm}^{-1}$  on KBr phase. UV–vis diffuse reflectance spectra were recorded on a Shimadzu UV–2100 recording spectrophotometer in the range 200–800 nm. The specific surface area of the catalysts were determined by BET method by nitrogen adsorption at  $-197^\circ\text{C}$  using a Micromeritics Flow Prep-060 instrument. Thermal analyses were performed by taking 10 mg of samples at a heating rate of  $10^\circ\text{C}/\text{min}$  on a Seiko TG V15 Dupont 2100 instrument in air (30 ml/min). The size and morphology of the prepared catalysts were estimated by scanning electron microscope (Jeol Model 5200). Temperature programmed desorption was carried out to determine the strength of acid sites and the total acidity of the catalysts using ammonia as a probe adsorbate. In a typical experiment, 100 mg of the catalyst was placed in a tubular reactor and heated to  $200^\circ\text{C}$  under nitrogen flow for approximately 4–5 h. The reactor was then cooled and the adsorption of ammonia was conducted by exposing the sample to ammonia at a flow rate of 10 ml/min for 1 h. The acid strength distribution was then subsequently determined by raising the temperature in steps viz. 100–200, 200–300, 300–400 and 400– $500^\circ\text{C}$ , with the flow of nitrogen.

### 2.3. Catalytic experiments

#### 2.3.1. Hydroxylation of phenol

The hydroxylation reaction was performed batch wise in a double-necked 50 ml round bottom flask using phenol (2.8 g, 0.0298 mol), water (5 g) and 0.1 g of activated catalyst at a temperature of  $80^\circ\text{C}$ . At the beginning of the reaction, 30 wt.%  $\text{H}_2\text{O}_2$  (0.008 mol) was added in one lot, followed by heating the mixture to the required reaction temperature. The course of the reaction was followed by analyzing the reaction mixture periodically using a gas chromatograph (HP 6890) equipped with a flame ionization detector (FID) and a capillary column (5  $\mu\text{m}$  cross-linked methyl silicone gum, 0.2 mm  $\times$  50 m) and by injecting authentic samples.

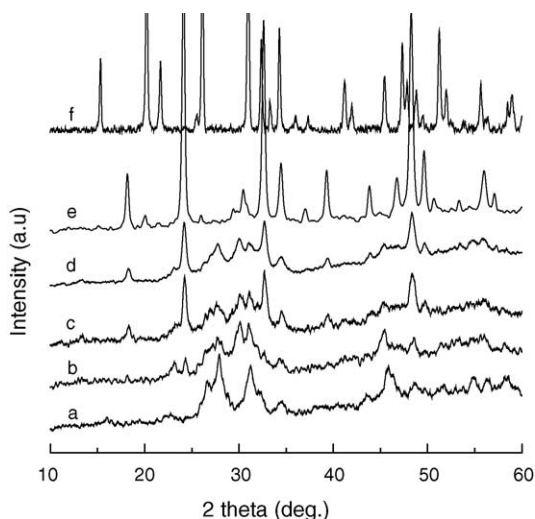


Fig. 1. Powder XRD patterns of  $V_2O_5$ - $Nd_2O_3$  catalysts calcined at  $500^\circ C$ : (a) 0VN/500, (b) 6VN/500, (c) 9VN/500, (d) 15VN/500, (e)  $NdVO_4$  and (f)  $V_2O_5$ .

### 3. Results and discussion

The powder X-ray diffractograms of the support,  $V_2O_5$ - $Nd_2O_3$  catalysts of various vanadia loadings and reference  $NdVO_4$ ,  $V_2O_5$  calcined at  $500^\circ C$  are given in Fig. 1. The formation of higher vanadate species were checked by comparison of the vanadia loaded catalysts with the  $NdVO_4$  prepared and the existence of additional peaks at higher loadings indicates the co-existence of vanadia and neodymia phases. The support neodymia calcined at  $500^\circ C$  exhibits poor crystallinity and the broad diffraction peaks observed might be due to  $Nd_2O_3$  phases and with an increase in the percentage of vanadia loading the phase crystallinity gets increased, while the XRD patterns of  $NdVO_4$  is very sharp and intense indicating the complete formation of crystalline orthovanadate phases. An interesting feature is that the intensity of the peaks at  $2\theta$ , 24.2, 32.7 and 48.5 ascribed to the formation of tetragonal orthovanadate phase [20], appears after a 9 wt.% incorporation of vanadia and its intensity gets increased with further vanadia loading. The peak at  $2\theta$ , 20.2 corresponding to  $V_2O_5$  is not observed even for higher loadings which suggests that an amorphous or a highly dispersed state of  $V_2O_5$  on the surface of the support or the crystallites formed are less than 4 nm in size that is beyond the detection capability of the XRD technique. Thus, the absence of any  $V_2O_5$  or orthovanadate peaks at lower loadings, is a clear indication that vanadia exists in a highly dispersed state on the support surface. In order to investigate the influence of calcination temperature on the dispersion of  $V_2O_5$ , XRD patterns are also taken for catalysts calcined at  $700^\circ C$ . Interestingly, no additional phases of  $V_2O_5$  are formed with an increase in the calcination temperature, but the peaks characteristic of  $Nd_2O_3$  gets broadened and slightly modified (Fig. 2).

FTIR spectra of  $Nd_2O_3$ ,  $V_2O_5$ - $Nd_2O_3$ ,  $NdVO_4$  and  $V_2O_5$  catalysts were recorded after calcination at  $500^\circ C$ , in or-

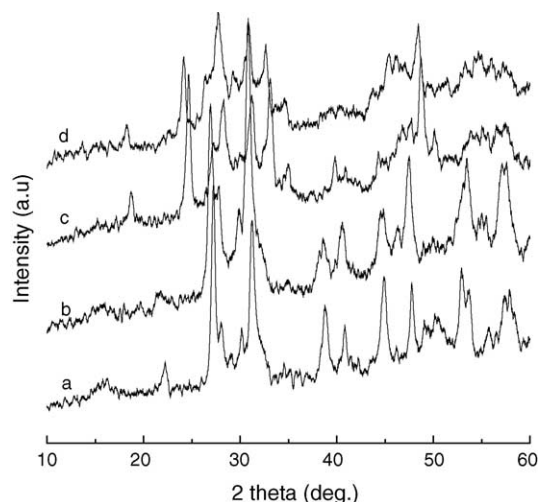


Fig. 2. Powder XRD patterns of  $V_2O_5$ - $Nd_2O_3$  catalysts calcined at  $700^\circ C$ : (a) 0VN/500, (b) 6VN/500, (c) 9VN/500 and (d) 15VN/500.

der to avoid the weakly adsorbed atmospheric species like carbonates, hydroxyls and water from the catalyst surface (Fig. 3). The spectra of the support shows sharp peaks at  $1475$ ,  $1095$ ,  $856\text{ cm}^{-1}$  and in the region of  $3500$ – $3200\text{ cm}^{-1}$ , while the reference  $NdVO_4$  shows a broad band in the range of  $810$ – $780\text{ cm}^{-1}$  with sharp peaks at  $1018$ ,  $1363$  and  $1510\text{ cm}^{-1}$ . The peak observed at  $1018\text{ cm}^{-1}$  for  $NdVO_4$  results from the  $V=O$  stretching of the vanadium oxide species, since pure  $V_2O_5$  shows its characteristic peak at  $1020\text{ cm}^{-1}$  and at  $820\text{ cm}^{-1}$  attributed to the  $V=O$  stretching and  $V-O-V$  deformation modes [21] and hence considered as an impurity. The prominent and intense band observed at higher loadings in the range of  $790$ – $770\text{ cm}^{-1}$  can be accounted for the

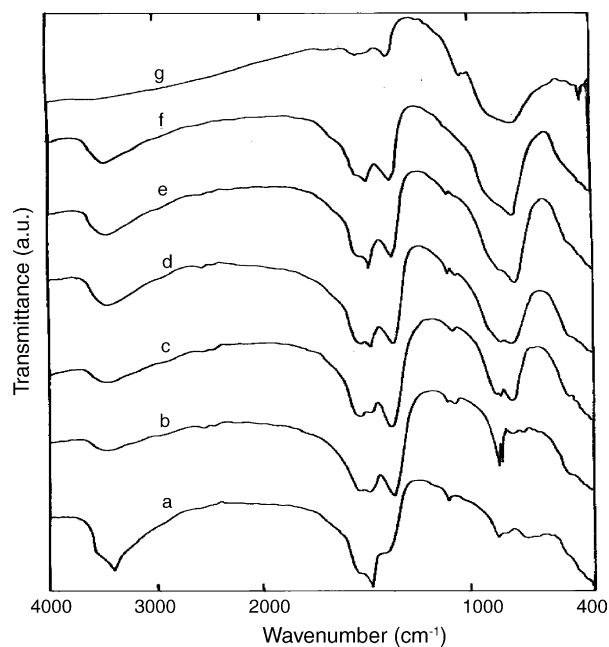


Fig. 3. FTIR spectra of: (a) 0VN/500, (b) 3VN/500, (c) 6VN/500, (d) 9VN/500, (e) 15VN/500, (f)  $NdVO_4$  and (g)  $V_2O_5$ .

presence of orthovanadate species [22]. In detail, the band at  $792\text{ cm}^{-1}$  is due to the asymmetric stretching of  $\text{VO}_4^{3-}$  ( $\nu_{\text{as}}(\text{VO}_4)$ ) entity, from orthovanadate species, and the peak at  $445\text{ cm}^{-1}$  is due to the symmetric stretching of  $\text{VO}_4^{3-}$  ( $\nu_{\text{s}}(\text{VO}_4)$ ). Broadening of these bands with vanadia loading indicates a stronger interaction between vanadia species and the support surfaces. Furthermore, formation of the orthovanadate phases at higher loadings may be due to the interaction of the isolated vanadate species with the support neodymia to form the stable  $\text{NdVO}_4$ . These results are in accordance with Deo and Wachs [23] who reported that the stabilization of vanadate species depends on the nature of acid–base properties of supports and on the vanadia concentrations. For instance, a bidimensional vanadate species is formed by the interaction of vanadia with basic  $\text{MgO}$  while its interaction with  $\text{SiO}_2$  does not lead to any compound formation. In other words, on acidic supports V–O–V polymers and on basic supports pyro or orthovanadates are preferentially formed. In the hydroxyl region ( $3600\text{--}3000\text{ cm}^{-1}$ ), the broad band centered around  $3440\text{ cm}^{-1}$  is accounted for the presence of surface hydroxyl groups and a slight decrease in intensity of these bands with the percentage of vanadia shows some sort of interaction of the surface hydroxyls with vanadia. In line with the XRD results, no peaks characteristic of the  $\text{V}_2\text{O}_5$  species are observed for all the  $\text{V}_2\text{O}_5\text{-Nd}_2\text{O}_3$  catalyst systems and hence it is reasonable to conclude that vanadia exist as highly dispersed species on the support surfaces at lower loadings and after the possible monolayer capacity it may get stabilized in the form of higher orthovanadate species. Further, the absence of crystalline  $\text{V}_2\text{O}_5$  species in all the supported catalyst systems is confirmed from the Raman analysis (figure not shown). Moreover, formation of any polyvanadyl surface species is ruled out, since they manifest V=O stretching frequencies in  $1000\text{--}950\text{ cm}^{-1}$  region [24].

The results obtained from the surface area analysis summarized in Table 1 shows that the specific surface area of the support and the vanadia-loaded catalysts are low and are in the range  $24\text{--}7\text{ m}^2\text{ g}^{-1}$ . A consistently decreasing trend in the surface area is observed while increasing the loading of  $\text{V}_2\text{O}_5$ . The initial loss in surface area and pore volume observed in the supported systems may be due to the penetration of the dispersed vanadium oxide into the pores of the support

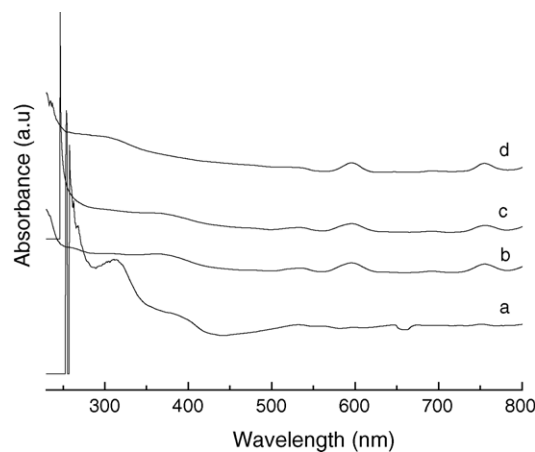


Fig. 4. Diffuse reflectance UV-Visible spectra of: (a) 0VN/500, (b) 6VN/500, (c) 12VN/500 and (d)  $\text{NdVO}_4$ .

and thereby narrowing its pore diameter and blocking some of its micro pores. The decrease in surface area of the support material is usually completed only after the formation of monolayer coverage of the active component impregnated. Thus, with an increase in the percentage of vanadia loading the surface area gets decreased and the decrease is more pronounced at higher loadings which further confirms the above explanation of the possible interaction of isolated vanadyl surfaces with the support to form the stable, larger orthovanadate species.

Diffuse reflectance UV–vis spectroscopy is often used to identify the oxidation states and coordination environments of transition metal ions in supported metal oxide or zeolite catalysts [25]. The spectrum visualized in Fig. 4 shows some important differences in the d–d and UV region of the  $\text{V}_2\text{O}_5\text{-Nd}_2\text{O}_3$  catalysts and the support. Generally, the spectra of pure  $\text{V}_2\text{O}_5$  shows strong absorptions in the UV region and gets extends to the visible region and are mainly associated to the charge transfer transitions from the O 2p valence band to the empty V 3d orbitals [26]. The bands in the range  $250\text{--}340\text{ nm}$  are very strong for the present  $\text{V}_2\text{O}_5\text{-Nd}_2\text{O}_3$  catalysts assigned to the presence of  $\text{V}^{5+}$  ions with a tetrahedral coordination but the bands in the range  $500\text{--}800\text{ nm}$  are weak, and are attributed to the d–d transitions of  $\text{V}^{4+}$  ( $d^1$ )

Table 1  
Physico-chemical properties and acid strength distribution of  $\text{V}_2\text{O}_5\text{-Nd}_2\text{O}_3$  catalysts

Catalyst	Surface area <sup>a</sup> ( $\text{m}^2\text{ g}^{-1}$ )	Pore volume ( $\text{cc g}^{-1}$ )	Crystal size <sup>b</sup> ( $\mu\text{m}$ )	$\text{NH}_3$ desorbed <sup>c</sup> ( $\text{mmol g}^{-1}$ )				Total acidity
				100–200 ( $^\circ\text{C}$ )	200–300 ( $^\circ\text{C}$ )	300–400 ( $^\circ\text{C}$ )	400–500 ( $^\circ\text{C}$ )	
0VN/500	24.80	0.0129	2.95	0.05	0.07	0.09	0.10	0.31
3VN/500	19.53	0.0059	–	0.10	0.13	0.16	0.12	0.51
6VN/500	17.72	0.0050	2.35	0.18	0.15	0.20	0.15	0.68
9VN/500	13.28	0.0043	2.15	0.24	0.18	0.20	0.20	0.82
12VN/500	10.15	0.0038	2.02	0.28	0.20	0.23	0.22	0.93
15VN/500	7.23	0.0031	–	0.31	0.23	0.24	0.27	1.05
$\text{NdVO}_4$	11.15	0.0068	0.42	0.21	0.16	0.20	0.18	0.75

<sup>a</sup> Measured by nitrogen adsorption–desorption at  $-197\text{ }^\circ\text{C}$ .

<sup>b</sup> Measured from SEM analysis (JOEL JSM-5200).

<sup>c</sup> Measured by TPD analysis using ammonia as adsorption–desorption agent.

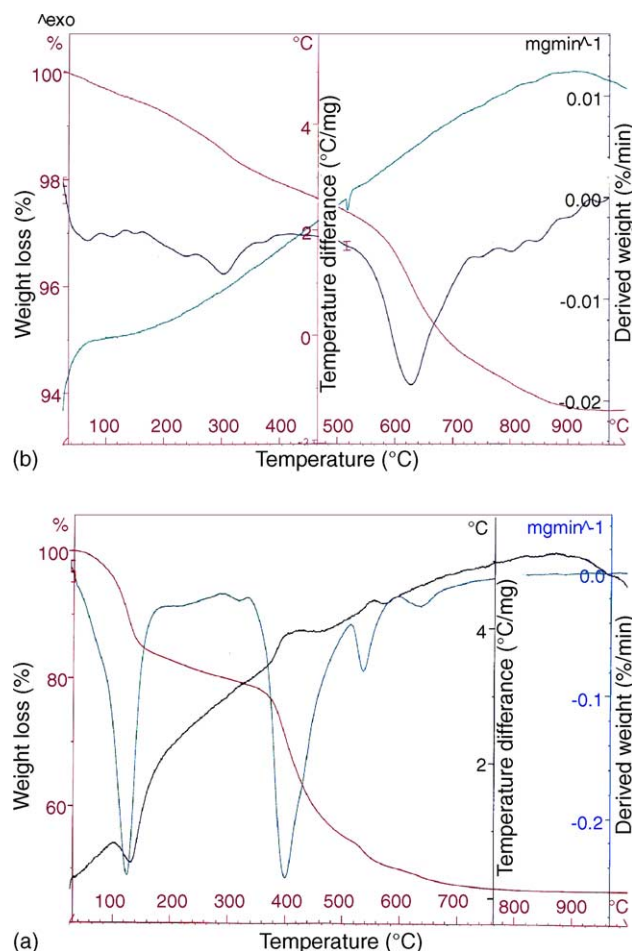


Fig. 5. Thermo gravimetric-differential thermal analysis (TG-DTG, DTA) plots of: (a) 3VN/100 and (b) 15VN/500.

ions [27]. Since  $\text{Nd}_2\text{O}_3$  reflects no peaks in the visible region, it is reasonable to assume that the formation of peaks in the visible region for  $\text{V}_2\text{O}_5\text{-Nd}_2\text{O}_3$  samples may contribute from the orthovanadate species, since the reference  $\text{NdVO}_4$  shows a same behaviour.

The TGA/DTA spectrum of as synthesized 3VN/500 and calcined 15VN/500 catalysts are given in Fig. 5. The initial weight loss observed for all samples from room temperature to 200 °C can be attributed to the loss of physisorbed water. The percentage weight loss of water in the support (figure not shown) and vanadia loaded samples is low which may be due to a fairly low specific surface area of the support and hence the surface population of hydroxyl groups was expected to be rather low. The DTG spectrum of the as synthesized 3VN/100 sample shows a strong weight loss around 400 °C, due to the transformation of the compound  $(\text{NH}_4)_2\text{O}(\text{V}_2\text{O}_5)_3$  into  $\text{V}_2\text{O}_5$  [28]. However, the DTG spectrum of the calcined 15VN/500 catalyst showed no weight loss till the temperature reached 600 °C and the observed weight loss in the region 500–800 °C may be due to the complete consumption of  $\text{V}_2\text{O}_5$  to form neodymium orthovanadates ( $\text{Nd}_2\text{O}_3 + \text{V}_2\text{O}_5 \rightarrow 2\text{NdVO}_4$ ). These types of results are

observed earlier for a  $\text{V}_2\text{O}_5/\text{CeO}_2$  system, where the weight loss observed in the range 500–800 °C is accounted for the departure of oxygen from the solid and for the formation of cerium orthovanadates ( $2\text{CeO}_2 + \text{V}_2\text{O}_5 \rightarrow 2\text{CeVO}_4 + 1/2\text{O}_2$ ) [29].

Temperature programmed desorption measurements of ammonia ( $\text{NH}_3$ -TPD) were carried out in steps to evaluate the acidic nature of the  $\text{V}_2\text{O}_5\text{-Nd}_2\text{O}_3$  catalysts, using ammonia as an adsorbate. Usually, the acidity of the solid acid catalysts were determined by the temperature programmed desorption studies using ammonia or pyridine as probe adsorbate molecules. The present acidity measurements were performed by using ammonia as a probe since almost all the acid sites present on the catalyst surface are easily accessible for the smaller ammonia molecules and hence a quantitative determination of the acid sites can be envisaged. The desorption of ammonia were verified in the temperature range of 100–200, 200–300, 300–400 and 400–500 °C and was found that the total acidity gets increased with increasing vanadium content (Table 1). Usually, the formation of surface vanadia species on oxide support is accompanied by a decrease in the surface Lewis acid sites and an increase in the number of Bronsted acid sites and the concept seems to be well for the present catalyst systems.

## 4. Catalytic activity results

### 4.1. Phenol hydroxylation

Hydroxylation of phenol was carried out as a model reaction, to determine the relative reactivities of  $\text{V}_2\text{O}_5\text{-Nd}_2\text{O}_3$  catalysts. The results of phenol hydroxylation reaction given in Table 2, shows that the nature of vanadium species had a deciding role in the conversion and selectivity for mono hydroxylated products. The enhanced catalytic activity of lower vanadia loaded catalysts, especially 3VN/500, is an indirect evidence for a better dispersion of the active vanadia species on the support or for the presence of isolated surface vanadyl sites, which may helps in the chemisorption of  $\text{H}_2\text{O}_2$  with

Table 2  
Catalytic activity and selectivity observed in phenol hydroxylation by  $\text{H}_2\text{O}_2$  over various  $\text{V}_2\text{O}_5\text{-Nd}_2\text{O}_3$  catalysts<sup>a</sup>

Catalyst	Phenol conversion (%)	Product distribution (%) <sup>b</sup>		
		CAT	HQ	BQ
0VN/500	2.8	100	–	–
3VN/500	12.0	65.3	28.9	5.8
6VN/500	9.9	56.2	35.1	8.7
9VN/500	7.4	47.0	42.1	10.9
12VN/500	4.9	45.6	19.9	34.5
15VN/500	3.6	40.6	23.1	36.3
$\text{NdVO}_4$	4.7	48.2	45.3	6.5

<sup>a</sup> Reaction conditions:  $T=80^\circ\text{C}$ ;  $t=6\text{ h}$ ; substrate/oxidant = 3; catalyst = 3.6% of substrate, solvent ( $\text{H}_2\text{O}$ ) = 5 g.

<sup>b</sup> CAT, catechol; HQ, hydroquinone; BQ, benzoquinone.

Table 3

Catalytic activity and selectivity observed in phenol hydroxylation by H<sub>2</sub>O<sub>2</sub> over 3VN/500 catalyst with various reaction times<sup>a</sup>

Reaction time (h)	Phenol conversion (%)	Product distribution (%)		
		CAT	HQ	BQ
1	3.8	63.1	32.6	4.3
3	7.6	65.3	27.2	7.5
5	10.1	66.3	23.8	9.9
6	12.0	65.3	28.9	5.8
9	14.1	63.6	33.1	3.3

<sup>a</sup> Other reaction conditions: see footnotes of Table 2.

ease. Thus, the catalysts having vanadium species well dispersed on the support surface are more active than the higher coordinated orthovanadates or bulk V<sub>2</sub>O<sub>5</sub> catalysts.

It is well known that the formation of hydroxylation products and its selectivity depends upon reaction temperature, molar ratio, nature of solvent and reaction time. Increase in reaction time and reaction temperature helps to increase the catechol (CAT) selectivity and at the same time the selectivity for benzoquinone (BQ) gets decreased which may be due to the over oxidation of the formed benzoquinone to tar, as observed in case of TS-1 catalysts [30]. For instance, the catalyst 3VN/500 shows a BQ selectivity of 9.9% at 5 h, which after 6 h gets decreased to 5.8% assigned to the above explanation of the over oxidation of the formed BQ to tar. Table 3 further illustrates the conversion and selectivity observed over 3VN/500 catalyst as a function of time. Even though the conversion gets slightly improved at longer reaction time, viz. 9 h, the further oxidation of benzoquinone to tarry materials limits the present reaction time as 6 h. Further, in order to study the influence of reaction temperature, the catalyst 3VN/500 was also screened over a broad temperature range of 60–90 °C and the results obtained are given in Table 4. Obviously, an increased reaction temperature of 80 °C helps to increase the phenol conversion significantly. However, a further increase in temperature, viz. 90 °C, shows a sharp decrease in phenol conversion due to the fast decomposition of H<sub>2</sub>O<sub>2</sub>, with an increase in BQ selectivity. These results show that an increase in temperature above 80 °C accelerates only the oxidation of HQ to BQ and the subsequent oxidation of BQ to tarry materials. Hence, the optimum temperature for the present reaction was opted as 80 °C. As a further optimization, the activity of the catalyst was screened over different solvents, since various detailed studies over

Table 4

Catalytic activity and selectivity observed in phenol hydroxylation by H<sub>2</sub>O<sub>2</sub> over 3VN/500 catalyst under various reaction temperatures<sup>a</sup>

Temperature (°C)	Phenol conversion (%)	Product distribution (%)		
		CAT	HQ	BQ
60	5.7	66.5	32.4	1.1
70	7.9	66.8	31.1	2.1
80	12.0	65.3	28.9	5.8
90	5.8	63.3	26.3	10.4

<sup>a</sup> Other reaction conditions: see footnotes of Table 2.

Table 5

Catalytic activity and selectivity observed in phenol hydroxylation by H<sub>2</sub>O<sub>2</sub> over 3VN/500 catalyst under various solvents<sup>a</sup>

Solvents	Phenol conversion (%)	Product distribution (%)		
		CAT	HQ	BQ
Water	12.0	65.3	28.9	5.8
Ethanol	5.6	61.5	37.7	0.8
Acetone	Inactive	–	–	–

<sup>a</sup> Other reaction conditions: see footnotes of Table 2.

titanium and vanadium containing zeolites shows that solvents had a profound influence on phenol conversion and further in its selectivities towards the monohydroxylated products [30,31]. Hence, careful investigation on the influence of various solvents reveals that the present catalysts are inactive in the commonly used solvent over TS-1 catalysts, viz. acetone (Table 5). But changing the solvent from organic to water results in an enhancement in phenol conversion and a reduction in the tar formation, as reported by Xiao et al. [32]. This discrepancy results from the polarity difference between the two solvents that phenol conversion increases with the polarity of the solvent, hence water being more polar than acetone gives a higher conversion.

Reaction data shows that the support is active under the present reaction conditions while pure V<sub>2</sub>O<sub>5</sub> gives only tarry materials under the same conditions due to over oxidation processes, since if no hydroxylation took place no tar formation was observed and the reaction mixture remains almost colourless [31]. So, we assumed that either a synergistic effect between the two-oxidation catalysts neodymia and vanadia or the chemisorption of H<sub>2</sub>O<sub>2</sub> on the isolated vanadyl species, which can react easily with phenol to form diphenols, might promote the reaction. Moreover, the stability of the peroxo complexes depends on the nature of the solvent/nature of the ligand bonded to the metal and the difference in it causes the variation in the catalytic properties [33]. Interestingly, the conversion of the reference compound NdVO<sub>4</sub> is higher than 15VN/500 catalyst, which may result from the low acidity of the catalysts since it is known that in liquid phase oxidation reactions the catalyst need the absence of certain sites such as acid sites in order to avoid undesirable side reaction. But with the percentage of vanadium loading, acidic sites become prominent and thus results in the formation of unwanted tarry materials. In the absence of catalyst, no phenol conversion was observed from blank experiments and also not significantly enhanced by increasing the catalyst amount (g cat/g phenol). Recycling of the catalyst shows that the activity of the catalyst remains almost constant, even after three runs, and thus points that the catalyst is stable and can be extended towards various oxidation reactions.

## 5. Conclusions

In short, a series of neodymia supported vanadia catalysts are prepared and were characterized in detail by various

physicochemical techniques. Preliminary characterization data reveals the presence of two kinds of vanadia species on the support surfaces—one in the form of a highly dispersed vanadia species at low loadings and the other as an orthovanadate species at higher loadings and had shown its impact on the reaction studied. Unlike other rare-earth vanadium oxide systems (La–V–O), where several mixed phases are formed, Nd–V–O catalysts specifically form orthovanadate species at higher loadings and may be due to the large stabilization energy of the formed NdVO<sub>4</sub> species. Further investigations are going on to disclose the exact mechanism of the interaction of different vanadium sites with the support and are quite applicable, since the phases obtained with neodymia are similar to a Ce–V–O catalyst.

### Acknowledgements

We are grateful to Dr. Thomas Mathew and Mr. B.M. Devassy for useful discussions. S.S. and S.R.K. thanks C.S.I.R., India, for research fellowships.

### References

- [1] J.G. Eon, R. Olier, J.C. Volta, *J. Catal.* 145 (1994) 318.
- [2] H.H. Kung, M.C. Kung, *Appl. Catal. A* 157 (1997) 105.
- [3] A. Khodakov, B. Olthof, A.T. Bell, E. Iglesia, *J. Catal.* 181 (1999) 205.
- [4] I.E. Wachs, R.Y. Saleh, S.S. Chan, C.C. Chersch, *Appl. Catal. A* 15 (1985) 339.
- [5] H. Bosch, F. Janssen, *Catal. Today* 2 (1988) 369.
- [6] B.M. Reddy, A. Khan, Y. Yamada, T. Kobayashi, S. Loridant, J.-C. Volta, *J. Phys. Chem. B* 106 (2002) 10964.
- [7] J. Matta, D. Courcot, E.A. Aad, A. Aboukais, *Chem. Mater.* 14 (2002) 4118.
- [8] C.T. Au, W.D. Zhang, H.L. Wan, *Catal. Lett.* 37 (1996) 241.
- [9] C.T. Au, W.D. Zhang, *J. Chem. Soc. Faraday Trans.* 93 (1997) 1195.
- [10] A. Esposito, M. Taramasso, C. Neri, F. Byonomo, US Patent 4,396,783, 1983.
- [11] Y. Yu, J.F. Yu, T.H. Wu, C.X. Chin, *J. Catal.* 18 (1997) 230.
- [12] D.R.C. Huybrechts, *Catal. Lett.* 8 (1991) 273.
- [13] L.Y. Litvintsu, *Kinet. Catal.* 34 (1993) 71.
- [14] M. Ai, *J. Catal.* 54 (1978) 223.
- [15] T.A. Tatarinova, *Kinet. Katal.* 23 (1985) 54.
- [16] S. Goldstein, G. Czapski, J. Robani, *J. Phys. Chem.* 98 (1994) 6586.
- [17] R.B. Yu, F.S. Xiao, D. Wang, J.M. Sun, R.R. Xu, *Catal. Today* 51 (1999) 39.
- [18] J.M. Sun, X.J. Meng, Y.H. Shi, F.S. Xiao, *J. Catal.* 193 (2000) 199.
- [19] V. Venkat Rao, K.V. Narayana, A. Venugopal, K.S. Rama Rao, S. Khaja Masthan, P. Kanta Rao, *Appl. Catal. A* 150 (1977) 269.
- [20] C.T. Au, W.D. Zhang, *J. Chem. Soc. Faraday Trans.* 93 (1997) 1195.
- [21] G. Busca, G. Centi, L. Marchetti, F. Trifiro, *Langmuir* 2 (1986) 568.
- [22] J.A. Gadsen, *IR Spectra of Minerals and Related compounds*, 1975.
- [23] G. Deo, I.E. Wachs, *J. Phys. Chem.* 95 (1991) 5889.
- [24] L.D. Frederickson Jr., D.M. Hausen, *Anal. Chem.* 35 (1963) 818.
- [25] G. Catana, R.R. Rao, B.M. Weckhuysen, P. Van der Voort, E. Vansant, R.A. Schoonheydt, *J. Phys. Chem. B* 102 (1998) 8005.
- [26] G. Centi, S. Perathoner, F. Trifiro, A. Aboukais, F. Aissi, M. Guelton, *J. Phys. Chem.* 96 (1992) 2617.
- [27] A. Corma, J.M. Lopez Nieto, N. Paredes, *Appl. Catal. A* 104 (1993) 161.
- [28] Z. Liu, W. Ji, L. Dong, Y. Chen, *Mater. Chem. Phys.* 56 (1998) 134.
- [29] R. Cousin, M. Dorrdin, E. Abi-Aad, D. Courcot, S. Capelle, M. Gueiton, A. Aboukais, *J. Chem. Soc. Faraday Trans.* 93 (1997) 3863.
- [30] J.A. Martens, Ph. Buskens, P.A. Jacobs, *Appl. Catal. A* 99 (1993) 7.
- [31] P.R.H. Prasad Rao, A.V. Ramaswamy, *Appl. Catal. A* 93 (1993) 123.
- [32] F.S. Xiao, J. Sun, X. Meng, R. Yu, H. Yuan, J. Xu, T. Song, D. Jiang, R. Xu, *J. Catal.* 199 (2001) 273.
- [33] H. Mimoun, L. Saussine, E. Daire, M. Postel, J. Fischer, R. Weiss, *J. Am. Chem. Soc.* 105 (1983) 3101.